Supporting Information

Self-assembled and well separated B and N co-doped hierarchical carbon structures as high-capacity, ultra-stable, LIB anode materials

Jinliang Zhu, Pengcheng Wei, Julian Key, Shibin Yin, Shaojian Ma and Pei Kang Shen**

Collaborative Innovation Center of Renewable Energy Materials, Guangxi Key Laboratory of Processing for Non-Ferrous Metal and Featured materials, Guangxi Key Laboratory for Electrochemical Energy Materials, Guangxi University, Nanning 530004, PR China.

*Corresponding author E-mail: jlzhu@gxu.edu.cn (J. Zhu); stsspk@mail.sysu.edu.cn (P. Shen). Fax: +86 07713237990, Tel: +86 07713237990.

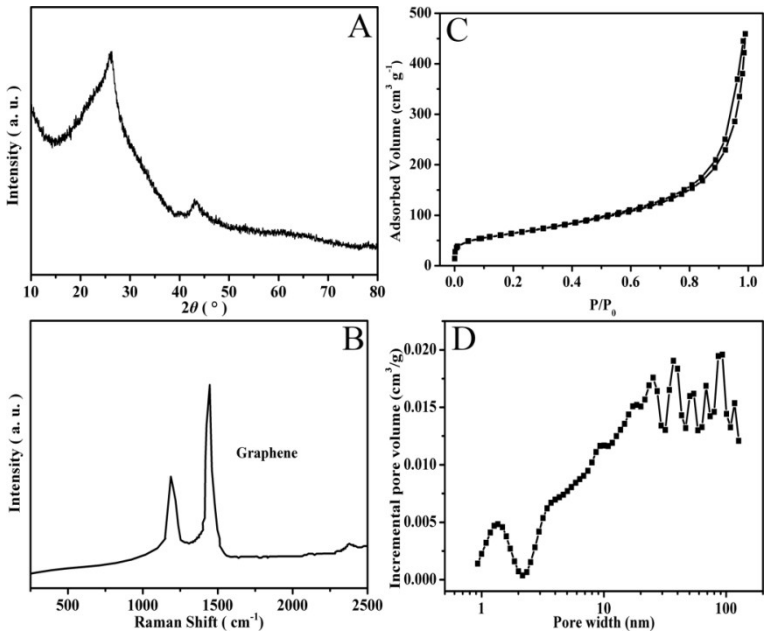

Fig. S1 (A) XRD pattern, (B) Raman spectrum, (C) N_2 adsorption-desorption isotherm and (D) pore size distribution curve of commercial graphene

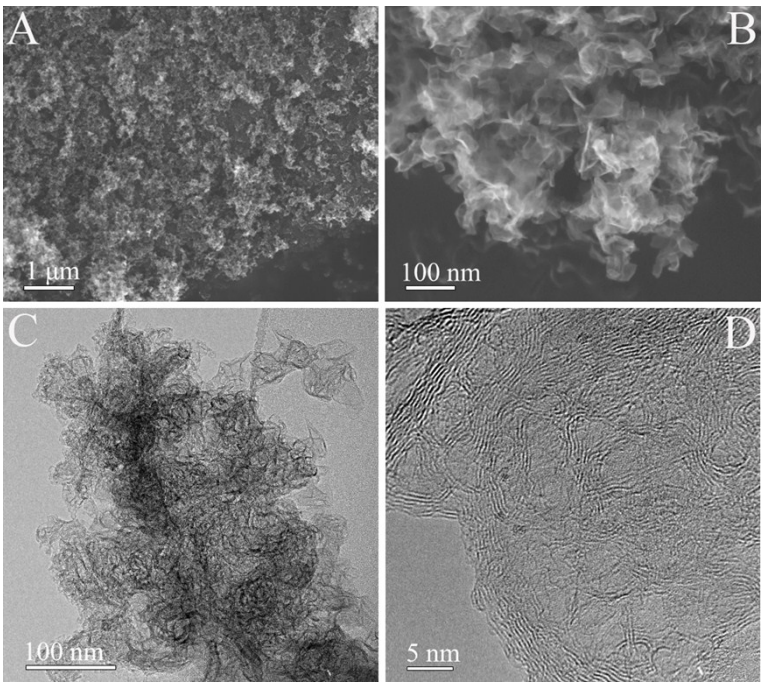

Fig. S2 (A, B) SEM and (C, D) TEM images of commercial graphene

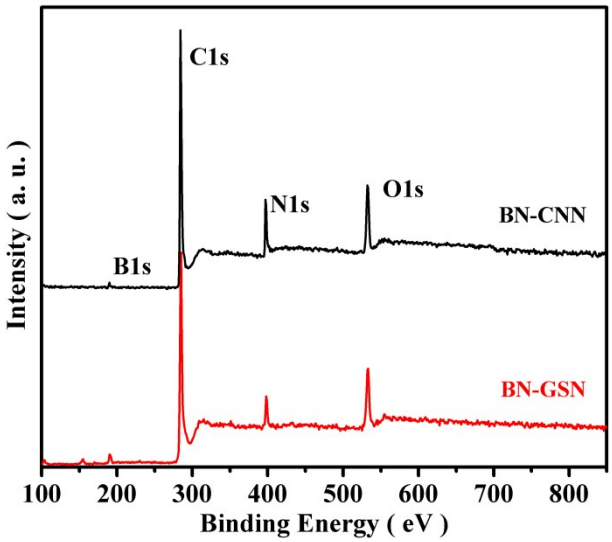

Fig. S3 XPS spectra of BN-CNN and BN-GSN

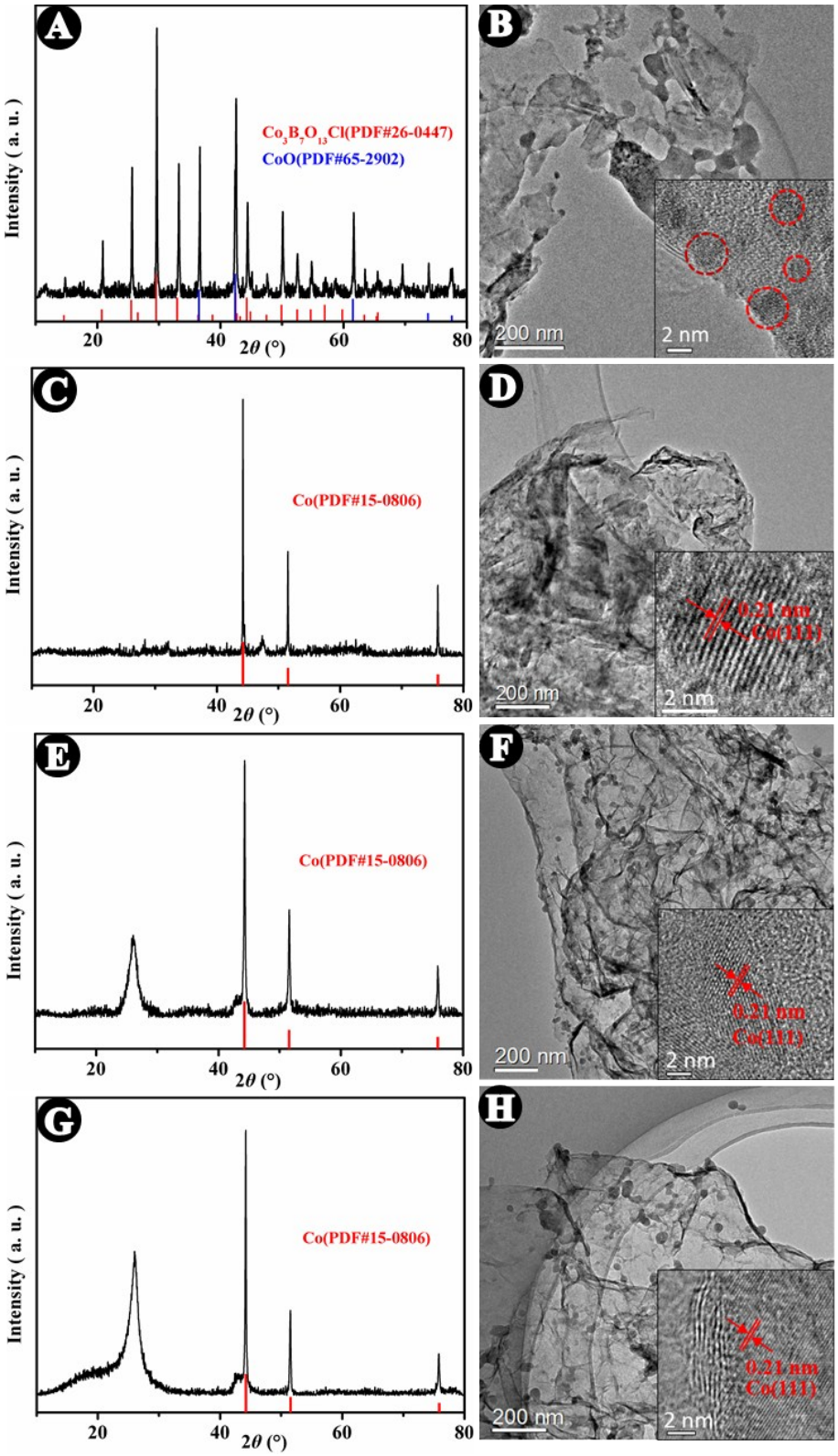

Fig. S4 XRD patterns and TEM images of BN-GSN at different temperatures: (A, B) 450 °C, (C, D) 600 °C, (E, F) 900 °C, and (G, H) 1000 °C.

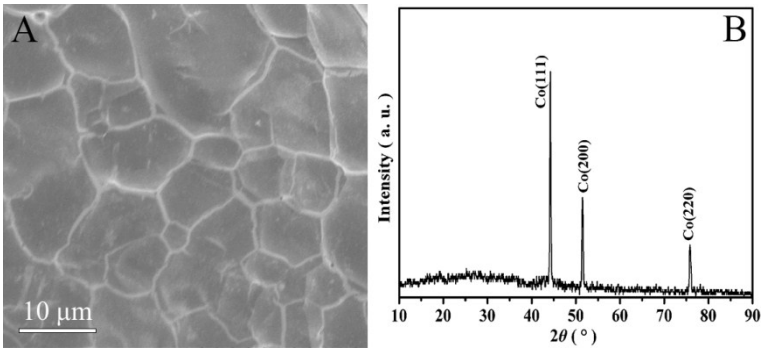

Fig. S5 (A) TEM image and (B) XRD pattern of cobalt foil at 450 °C

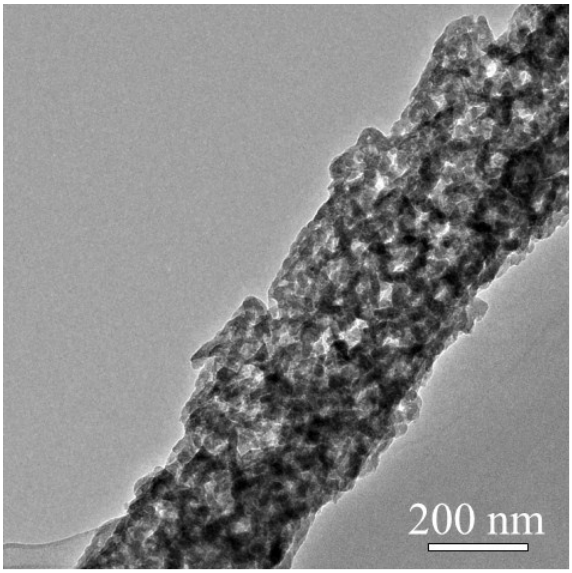

Fig. S6 Enlarged SEM image (Fig.5E) of growing BN-CNN

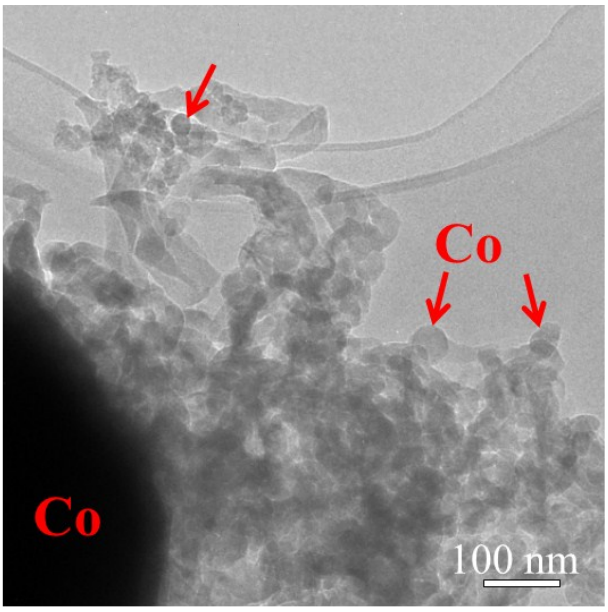

Fig. S7 Enlarged TEM image (Fig.5E) of growing BN-CNN

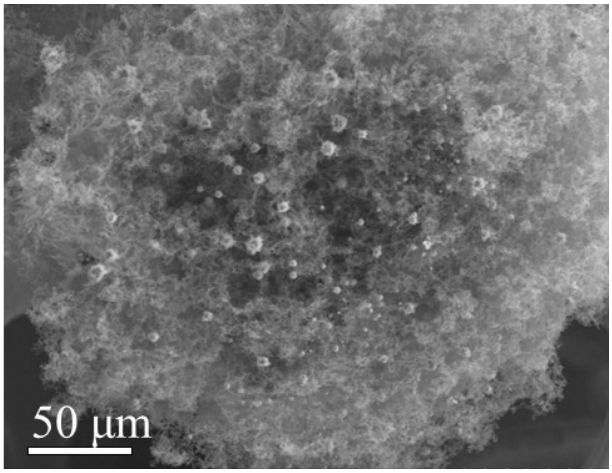

Fig. S8 SEM image of BN-CNN

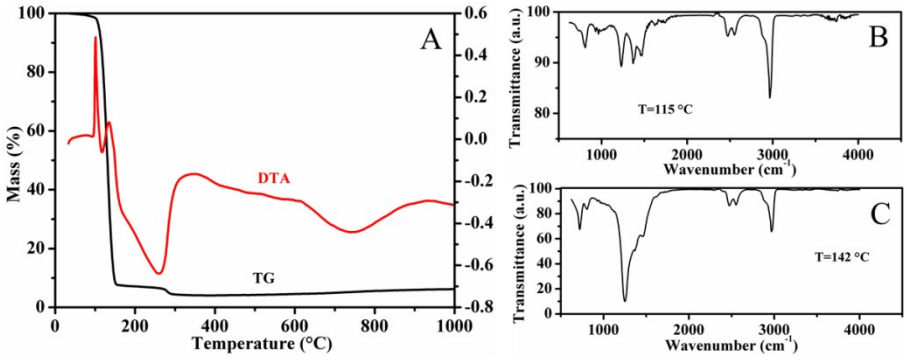

Fig. S9 (A) TG-DTA of *tert*-butylamine borane in N_2 from 25 °C to1000 °C and (B, C) FTIR spectra of the corresponding pyrolysis products at 115 and 142 °C, respectively.

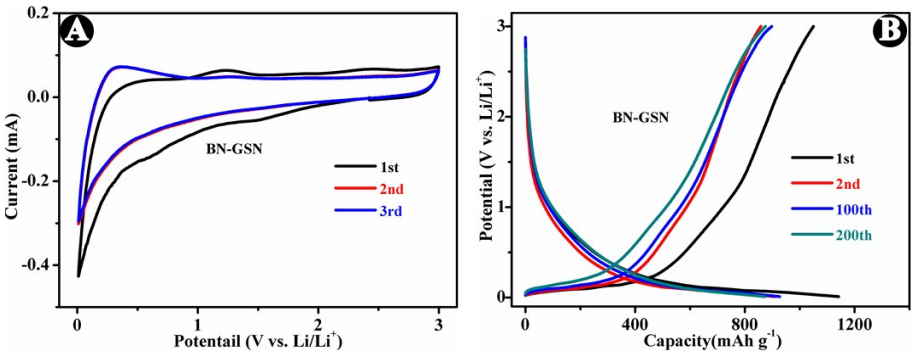

Fig. S10 (A) Cyclic voltammetry curves and (B) voltage profiles of BN-GSN in a voltage range from 0.01 V to 3 V (vs Li/Li^+)

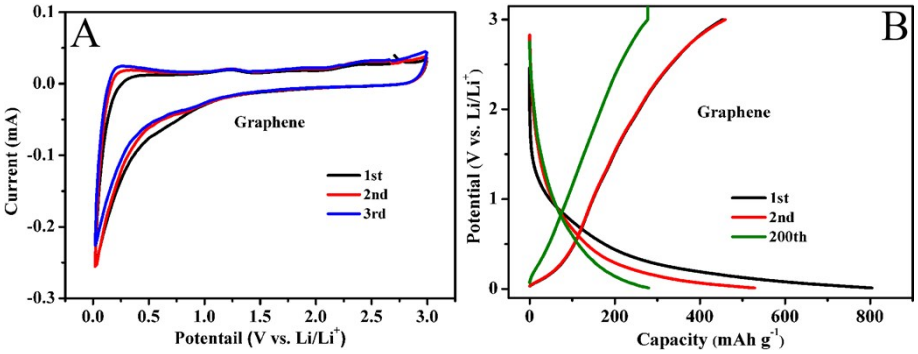

Fig. S11 (A) Cyclic voltammetry curves and (B) voltage profiles of commercial graphene in a voltage range from 0.01 V to 3 V (vs Li/Li^+)

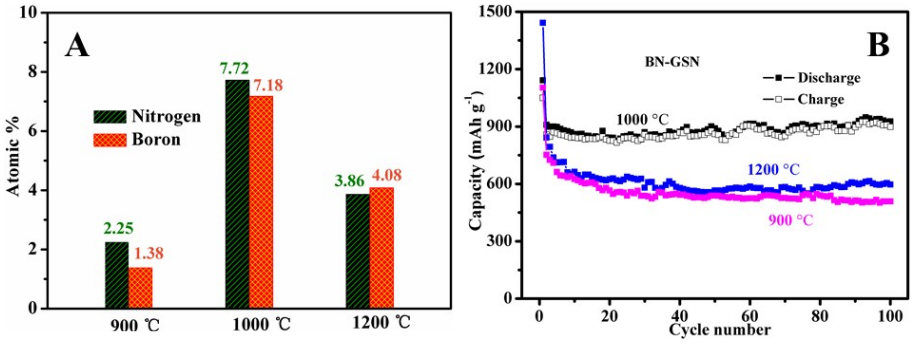

Fig. S12 (A) Surface atomic ratios and (B) Cycle behaviors at 50 mA/g of BN-GSN (900), BN-GSN (1000) and BN-GSN (1200)

Table S1 Electrolyte resistances and charge transfer resistances according to Nyquist plots of BN-CNN, BN-GSN, commercial graphene and graphite

Sample	R_e (Ω)	R_{ct} (Ω)
BN-CNN	2.3	3.8
BN-GSN	2.2	8.9
Graphene	2.5	14.4
Graphite	2.9	30.1

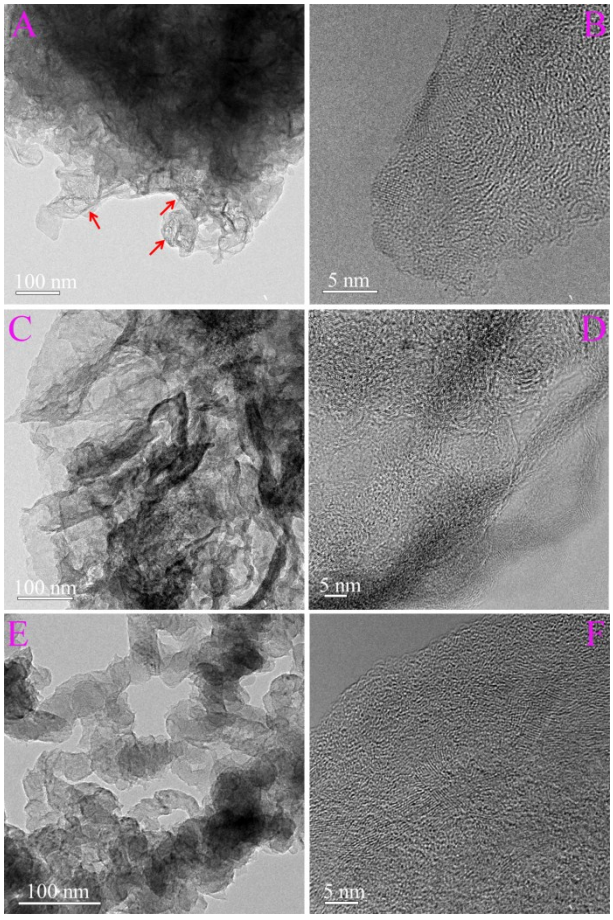

Fig. S13 (A) TEM and HRTEM of commercial graphene (A, B), BN-GSN (C, D) and BN-CNN (E, F) after 200 cycles at 0.05 A g^{-1}.

Table S2 Electrochemical performance of carbonaceous LIB anode materials

Materials	Preparation strategy	BET (m^2/g)	Rate (mA/g)	First cycle coulombic efficiency	Reversible capacity (mAh/g)	Capacity decay per cycle
N-Doped CNFs[1]	Electrospinning, urea treatment	381	30	82.8%	445	0.16%
N-Doped CNFs[2]	Oxidative template assembly	---	100	64.0%	668	0.94%
Porous CNFs[3]	Electrospinning, SiO_2 template	950	50	47.7%	730	0.78%
CNFs-CNTs[4]	Chemical vapor deposition, KOH activation	1840	100	～62.5%	1150	0.35%
N-doped Graphitic porous CNFs[5]	Electrospinning, Ni nanoparticle template	538	100	57.5%	1560	0.34%
Graphitic porous CNFs [6]	Electrospinning, Fe nanoparticle template	198	100	～60%	983	0.14%
N-Doped CNFs[7]	Chemical vapor deposition	108.1	37.2	60%	500.0	---
Porous CNFs[8]	Biomass method, KOH activation	1235.6	100	56%	1091.4	0.21%
Porous CNFs[9]	Electrospinning, air activation	583	50	---	1950	0.22%
N-doped graphene frameworks[10]	MgO nanowire template	610	200	52.3%	700	---
N-doped porous graphene[11]	Pyrolysis of graphene oxide/mela-mine–formaldehyde, Ice template	1170	100	58%	672	---
Porous graphene films[12]	Fe_3C nanoparticle template	36	50	～36%	1062	0.65%
Sulfur/nitrogen dual-doped porous graphene[13]	GO hydrothermal, thiourea treatment	624.5	50	75.99%	1109	0.23%

Graphene/N-doped carbon nanosheets[14]	Annealing Ppy/GO	327	100	57.3%	1100	0.20%
Carbon nanoparticles[15]	Soot deposition	133	100	55%	742	1.11%
CNTs@3DG[16]	Ni/Co catalyzing resin, KOH activation	1673	100	59%	1132	0.030%
Carbon nanosheets[17]	Petroleum asphalt NaCl/KCl	11	100	53.9%	729	---
HPCMs[18]	Carbonization of sucrose, MgAl-LDOs microsphere templates	852.7	50	54.52%	1140.5	0.18%
BN-CNN (This work)	Heat treatment, No extrinsic template	785	50 500	73.6%	1017 756	0.016% 0.017%

References

[1] S.-X. Wang, L. Yang, L.P. Stubbs, X. Li, C. He, ACS applied materials & interfaces, 5 (2013) 12275-12282.

[2] Z. Wang, X. Xiong, L. Qie, Y. Huang, Electrochimica Acta, 106 (2013) 320-326.

[3] D. Nan, J.-G. Wang, Z.-H. Huang, L. Wang, W. Shen, F. Kang, Electrochemistry communications, 34 (2013) 52-55.

[4] Y. Chen, X. Li, K. Park, J. Song, J. Hong, L. Zhou, Y.-W. Mai, H. Huang, J.B. Goodenough, Journal of the American Chemical Society, 135 (2013) 16280-16283.

[5] Y. Chen, X. Li, X. Zhou, H. Yao, H. Huang, Y.-W. Mai, L. Zhou, Energy & Environmental Science, 7 (2014) 2689-2696.

[6] B. Zhang, Z.-L. Xu, Y.-B. He, S. Abouali, M. Akbari Garakani, E. Kamali Heidari, F. Kang, J.-K. Kim, Nano Energy, 4 (2014) 88-96.

[7] X.-B. Cheng, Q. Zhang, H.-F. Wang, G.-L. Tian, J.-Q. Huang, H.-J. Peng, M.-Q. Zhao, F. Wei, Catal Today, 249 (2015) 244-251.

[8] W. Wang, Y. Sun, B. Liu, S. Wang, M. Cao, Carbon, 91 (2015) 56-65.

[9] W. Li, M. Li, M. Wang, L. Zeng, Y. Yu, Nano Energy, 13 (2015) 693-701.

[10] X. Jia, G. Zhang, T. Wang, X. Zhu, F. Yang, Y. Li, Y. Lu, F. Wei, Journal of Materials Chemistry A, 3 (2015) 15738-15744.

[11] Z.-Y. Sui, C. Wang, Q.-S. Yang, K. Shu, Y.-W. Liu, B.-H. Han, G.G. Wallace, Journal of Materials Chemistry A, 3 (2015) 18229-18237.

[12] X. Zhang, J. Zhou, C. Liu, X. Chen, H. Song, Journal of Materials Chemistry A, 4 (2016) 8837-8843.

[13] H. Shan, X. Li, Y. Cui, D. Xiong, B. Yan, D. Li, A. Lushington, X. Sun, Electrochimica Acta, 205 (2016) 188-197.

[14] X. Liu, J. Zhang, S. Guo, N. Pinna, Journal of Materials Chemistry A, 4 (2016) 1423-1431.

[15] R.R. Gaddam, D. Yang, R. Narayan, K. Raju, N.A. Kumar, X.S. Zhao, Nano Energy, 26 (2016) 346-352.

[16] S. Huang, J. Wang, Z. Pan, J. Zhu, P.K. Shen, Journal of Materials Chemistry A, 5 (2017) 7595-7602.

[17] Y. Wang, Y. Wang, J. Liu, L. Pan, W. Tian, M. Wu, J. Qiu, Carbon, 122 (2017) 344-351.

[18] L. Shi, Y. Chen, G. Chen, Y. Wang, X. Chen, H. Song, Carbon, 123 (2017) 186-192.